Supplementary Material for "How future changes in irrigation water supply and demand affect water security in a Mediterranean catchment"

J.P.C. Eekhout[a], I. Delsman[b], J.E.M. Baartman[b], M. van Eupen[c], C. van Haren[c], S. Contreras[d], J. Martínez-López[e,f], J. de Vente[a]

[a]*Soil and Water Conservation Research Group, CEBAS-CSIC, Murcia, Spain*
[b]*Soil Physics and Land Management Group, Wageningen University, Wageningen, the Netherlands*
[c]*Wageningen Environmental Research, Wageningen University & Research, Wageningen, the Netherlands*
[d]*FutureWater, Cartagena, Spain*
[e]*Department of Ecology, Faculty of Science, University of Granada, Granada, Spain*
[f]*Instituto Interuniversitario de Investigación del Sistema Tierra en Andalucía (IISTA), Universidad de Granada, Granada, Spain*

Contents of this file

Email address: joriseekhout@gmail.com (J.P.C. Eekhout)

Text S1: Irrigation water supply calculation

The irrigation water supply for irrigation consists of five sources, i.e. water supplied from groundwater, the Tagus-Segura Aqueduct, desalination, treated urban waste water and other sources (mainly water transferred from the Segura River catchment). The values used for desalination, treated urban waste water and other sources were based on the estimates from (MITECO, 2019). For water supplied from groundwater and the Tagus-Segura Aqueduct more literature sources were available. Here we discuss on which literature sources we base our estimation of irrigation water supply, accounting for an independent validation using irrigation water demand from the study area.

Groundwater

Groundwater extractions have been estimated at 58 $hm^3\ yr^{-1}$ by Confederación Hidrográfica del Segura (2023), 88.2 $hm^3\ yr^{-1}$ by MITECO (2019) and 104 $hm^3\ yr^{-1}$ by Jiménez-Martínez et al. (2016), indicating a lower and a higher limit for groundwater extraction in the study area. MITECO (2019) assumes a 25% loss due to desalination, which results in a lower limit of 43.5 $hm^3\ yr^{-1}$ and an upper limit of 78 $hm^3\ yr^{-1}$.

Tagus-Segura Aqueduct

Water transferred annually from the Tagus-Segura Aqueduct to the study area has been estimated at 49 $hm^3\ yr^{-1}$ by MITECO (2019). However, legally, the Campo de Cartagena should receive 122 $hm^3\ yr^{-1}$, which is 21.8% of the total water supply from the Tagus-Segura Aqueduct (560 $hm^3\ yr^{-1}$). Given this percentage and the actual average annual transfer to the Segura River catchment of 350 $hm^3\ yr^{-1}$ (Morote et al., 2017), the amount of water

transferred to the study area is estimated at 76.25 hm^3 yr^{-1}. This gives a lower limit of 49 hm^3 yr^{-1} and an upper limit of 76.25 hm^3 yr^{-1}.

Validation based on irrigation water demand

Given the water supplied by desalination, treated urban waste water and other sources as obtained from MITECO (2019), the total irrigation water supply from all sources ranges between 135.79 and 197.5 hm^3 yr^{-1} (Table S1).

Considering the irrigation water demand that were used for model calibration (i.e. 4678 and 3008 m^3 ha^{-1} for irrigated tree crops and horticulture, respectively; Soto-García et al., 2013) and the area covered by irrigation based on the 2020 land use map (i.e. 18156 and 39716 ha for irrigated tree crops and horticulture, respectively), the gross irrigation water demand is estimated at 204.4 hm^3 yr^{-1}. This estimate is closer to the upper limit of the total irrigation water supply, which was subsequently selected.

Table S1: The lower and upper limit of the irrigation water supply (hm^3 yr^{-1}) by the different sources in the study area.

Source	Lower limit	Upper limit
Groundwater	43.5	78
Tajus-Segura Aqueduct	49	76.25
Desalinisation	8.2	8.2
Treated urban waste water	24.09	24.09
Other sources	11	11
Total	135.79	197.54

Text S2: Nature-based Solutions

In SSP1, we implemented reduced tillage in combination with green manure (cover crops) in rainfed and irrigated agriculture. In the case of rainfed agriculture, cover crops will be planted in autumn and ploughed into the soil in early spring. In the case of irrigated agriculture, cover crops will be planted after harvest in the spring and ploughed into the soil just before the new crop cycle starts in the autumn. We used a parametrization of SLM practices in the SPHY-MMF model similar to Eekhout and de Vente (2019), in which soil organic matter in the root zone is increased with 31% (Aguilera et al., 2013; Almagro et al., 2016), the bulk density of the root zone is reduced with 4% (Aguilera et al., 2013), and a stem density of 500 stems m^{-2} and a stem diameter of 2.5 cm were assumed for the cover crops, as input for the soil erosion model.

In SSP1, we also assumed implementation of vegetated buffer strips, which represent a Nature-based Solution that is currently being implemented in the study area (BOE, 2020). The spatial distribution of the buffer strips was based on the following criteria: (1) on the hillslopes (i.e. an upstream area < 8 km^2), (2) sediment transport > 1 Mg yr^{-1}, and (3) only in agricultural areas. The guidelines for implementation of buffer strips provided by the regional ministry of agriculture suggest that the distance between buffer strips decreases with increasing slope (BOE, 2020). Hence, we implemented buffer strips on slope breaks, i.e. at 1% slope intervals from 1-5% and 0.5% slope intervals for slope >5%, which led to a total of 762 buffer strips in the study area. Buffer strips only affect the sediment transport in the SPHY-MMF model, which is parameterized by vegetation characteristics

that affect the roughness in the sediment transport routine. The guidelines for buffer strip implementation further specify a ground cover of 70-100% 2 years after implementation, hence, we assume a 85% ground cover. We based the other vegetation characteristics on the reduction of sediment transport with respect to a model run without buffer strips, using the land use map from the SSP1 scenario for the period 1991-2020. We calibrated the buffer strips vegetation parameters to obtain a reduction of 50% with respect to the baseline model run. The 50% reduction was based on the lower limit estimated by Arora et al. (2010). We specifically use the lower limit, because the guidelines suggest a buffer strip width of 1-3 m (BOE, 2020), which is also at the lower limit of recommended buffer strip widths (Prosser et al., 2020). These assumptions led to a stem density of 2125 stems m^{-2} and stem diameter of 0.02 m.

Text S3: Model description

SPHY-MMF (Terink et al., 2015; Eekhout et al., 2018) is forced by daily precipitation and temperature (average, minimum and maximum) data, for which the temperature data are used to determine the reference evapotranspiration through the Hargreaves equation (Hargreaves and Samani, 1985). The potential evapotranspiration is obtained by multiplying the reference evapotranspiration by the crop coefficient, which is obtained from a linear relationship with the Normalized Differenced Vegetation Index (NDVI) from the vegetation module. The vegetation module also determines the leaf area index (LAI), canopy storage and interception. The actual evapotranspiration is obtained by multiplying the potential evapotranspiration with a soil water deficit/surplus factor, which is a function of soil hydraulic properties, the current soil water content and plant-specific water need. Surface runoff is simulated by infiltration excess and saturation excess processes, where the former is obtained by a daily implementation of the Green-Ampt equation (Heber Green and Ampt, 1911) and the latter as a function of the current and saturated water content. The model accounts for three soil layers, i.e. root-zone, subzone and groundwater layer. Water can percolate from the root-zone to the subzone to the groundwater layer, while capillary rise may occur between the subzone and the root-zone. The total runoff consists of the sum of surface runoff, lateral flow from the root-zone and baseflow from the groundwater layer. Water is routed using a single flow algorithm, where a flow recession coefficient accounts for the flow delay from channel friction, which was used for model calibration.

Text S4: Model calibration

Calibration methods

The SPHY-MMF model was calibrated in the Rambla de Albujón subcatchment (Figure 1), which covers about 44% of the study area. The calibration consisted of four steps in which we calibrated (1) the irrigation module, (2) the hydrological modules, (3) the soil erosion module, and (4) the sediment transport module. Daily climate data for the model calibration was obtained from 45 precipitation and temperature stations surrounding the study area. The data were interpolated on a 5 km grid using the meteoland R package (De Cáceres et al., 2018) (R version 4.1.2). The irrigation and soil erosion modules were calibrated over the period 2001-2020. The discharge data used to calibrate the hydrological modules spanned the period 2016-2021 and the sediment yield data was obtained in the period 2003-2004. Hence, the calibration of the hydrological modules and sediment transport module was restricted to these two time periods.

Irrigation was applied for two types of crops, i.e. irrigated tree crops and irrigated horticulture. Year-round irrigation was assumed for irrigated tree crops. The land use map used in this study does not specify which crops belong to the irrigated horticulture class. However, the long-term averaged intra-annual NDVI timeseries shows that NDVI is highest in the period between September and April (Figure S1), from which we deduce that winter crops are most common in these areas. Lettuce is the most common winter crop in the study area (Soto-García et al., 2013), which is subsequently used for model parameterization. Within the model, irrigation was restricted to the period September 30 - April 23 for irrigated horticulture. The two irri-

gated crops were calibrated with irrigation water demand obtained from a survey among local farmers, which estimated irrigation water demand of 4678 m^3 ha^{-1} for irrigated tree crops and 3008 m^3 ha^{-1} for irrigated horticulture (Soto-García et al., 2013). Future land use scenarios also include reduced deficit irrigation (RDI), as a way to increase resource use efficiency. Two recent studies determined the relative change in irrigation water demand between full irrigation and reduced deficit irrigation, from which we estimated a relative reduction of 17% (Romero-Trigueros et al., 2020; Mira-García et al., 2023). Hence, we calibrated the irrigation module two times, first with the values obtained from Soto-García et al. (2013) for full irrigation, and second with a reduction of 17% for reduced deficit irrigation. The calibration of the irrigation module focused on the MAD model parameter, which was calibrated individually for the two irrigated crops classes. Optimal model parameter values were obtained by minimizing the PBIAS (percent bias).

In the second calibration step we calibrated the hydrological part of the model, with a focus on the daily discharge obtained at the catchment outlet for the period 2016-2021. Here we focused on several soil related model parameters, including the thickness of the rootzone and sub zone, the maximum allowable capillary rise between the sub zone and rootzone, and a flow recession coefficient. Optimal model parameter values were obtained by maximizing the Kling-Gupta Efficiency (KGE; Gupta et al., 2009) and minimizing the PBIAS. Due to the short period of the observed discharge, we were not able to use the discharge time series for model validation.

The third calibration step focused on the hillslope erosion estimates obtained from the soil erosion module. The calibration of the soil erosion rates

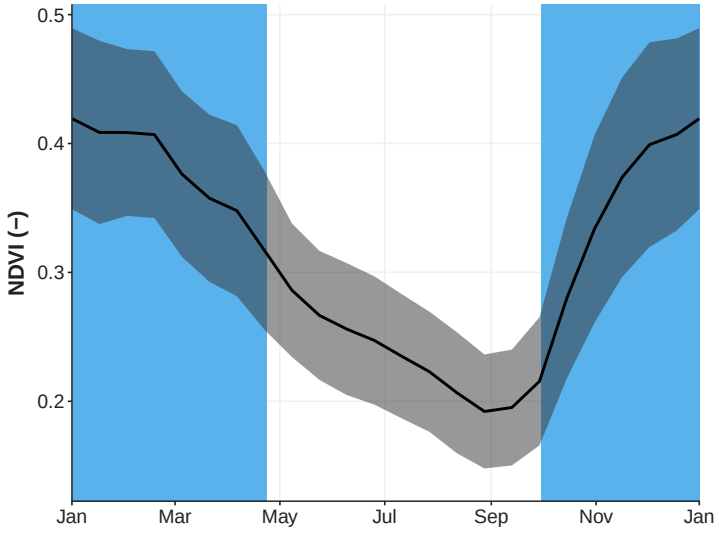

Figure S1: Long-term averaged (2009-2020) NDVI time series of the area covered by irrigated horticulture. The interval indicates the standard deviation around the mean. The period indicated with the blue background indicates the period when irrigation is applied in the SPHY-MMF model (i.e. 30/09 - 23/04).

was performed per land use class and compared to the plot-scale soil loss data for the Mediterranean region obtained from Maetens et al. (2012). We first calibrated the model parameters related to soil erodibility (K and DR) in the area covered by rainfed and irrigated tree crops. We focussed on tree crops because we assume that their ground cover is negligible due to frequent ploughing. Next, we calibrated the soil erosion rates for the three other land use classes, i.e. horticulture, forest, and shrubland, using land use specific model parameters, such as ground cover, stem diameter and stem density. Optimal calibration results were obtained when the difference between the literature hillslope erosion rates and the average simulated hillslope erosion

per land use class was smaller than 1%.

In the final calibration step, we calibrated the sediment yield at the catchment outlet, which was estimated to be 1863 Mg yr^{-1} for the period February 2003 - April 2004, according to García-Pintado et al. (2007). While we used the land use map obtained in 2020 for the other three steps, here we used a land use map obtained in 2000 (Carreño Fructuoso, 2015), which most likely better reflects the land use pattern for the period (2003-2004) in which the sediment yield data were obtained. The calibration focused on two model parameters (beta and gamma), which control the sediment transport within the SPHY-MMF model. Optimal model parameter values were obtained by minimizing the PBIAS (percent bias).

Calibration results

In the first step we calibrated the novel irrigation module separately for irrigated tree crops and irrigated horticulture. Calibration of full irrigation conditions, based on data obtained from Soto-García et al. (2013), resulted in MAD values of 1.267 for irrigated tree crops and 0.57 for irrigated horticulture (Table S2). This means that some plant water stress is allowed for irrigated tree crops ($MAD > 1$), while no plant water stress is allowed for irrigated horticulture ($MAD < 1$). Next, we calibrated the irrigation module for reduced deficit irrigation, assuming a reduction of 17.0% of the irrigation water demand obtained from Soto-García et al. (2013). This resulted in an increase of MAD values with respect to full irrigation, with 1.345 for irrigated tree crops and 1.08 for irrigated horticulture, which signifies that minor plant water stress is allowed for horticulture under reduced deficit irrigation.

In the second step, we calibrated the hydrological model using observed

Table S2: Irrigation properties used as SPHY-MMF model input. The irrigation technique include full irrigation (FI) and reduced deficit irrigation (RDI). The last column indicates the management allowable depletion (MAD).

Crop type	Irrigation technique	Start date	End date	MAD
Tree crops	FI	01/01	31/12	1.27
	RDI	01/01	31/12	1.345
Horticulture	FI	30/09	23/04	0.57
	RDI	30/09	23/04	1.08

discharge at the catchment outlet. We obtained optimal calibration results with a maximum capillary rise of 1.3 mm, a rootzone depth of 350 mm, a subzone depth of 300 mm and recession coefficient of 0.39. This resulted in a model efficiency of KGE = 0.84 and a PBIAS = 1.1% (Figure S2).

The soil erosion module was calibrated by first optimizing the soil erodibility parameters, which were multiplied by a factor of 1.77 to obtain optimal model efficiency for (irrigated and rainfed) tree crops. Optimal model efficiency for irrigated horticulture was obtained with a stem diameter of 0.14 m and a stem density of 25 stems m^{-2} (Table S3). For forest and shrubland, optimal model efficiency was obtained with a ground cover of 0.56 and 0.77, respectively. Finally, optimal model efficiency for sediment yield was obtained with beta = 1.785 and gamma = 1.34 from the sediment transport module.

Table S3: Model parameters for each land use class obtained for the irrigation and soil erosion modules. Where FI refers to full irrigation, RDI to reduced deficit irrigation, GC to ground cover, SDR to stem diameter and SDY to stem density. In the table, n/a means not applicable.

Land use class	GC (-)	Manning's n ($s\ m^{-1/3}$)	Stem diameter (m)	Stem density (stems m^{-2})
Irrigated tree crops	< 0.01	n/a	0.3	0.03
Irrigated horticulture	0.46	n/a	0.135	25
Rainfed tree crops	< 0.01	n/a	0.3	0.02
Greenhouses	0	n/a	n/a	n/a
Forest	0.56	0.2	n/a	n/a
Shrubland	0.77	0.1	n/a	n/a
Urban	0	n/a	n/a	n/a
Water	0	n/a	n/a	n/a

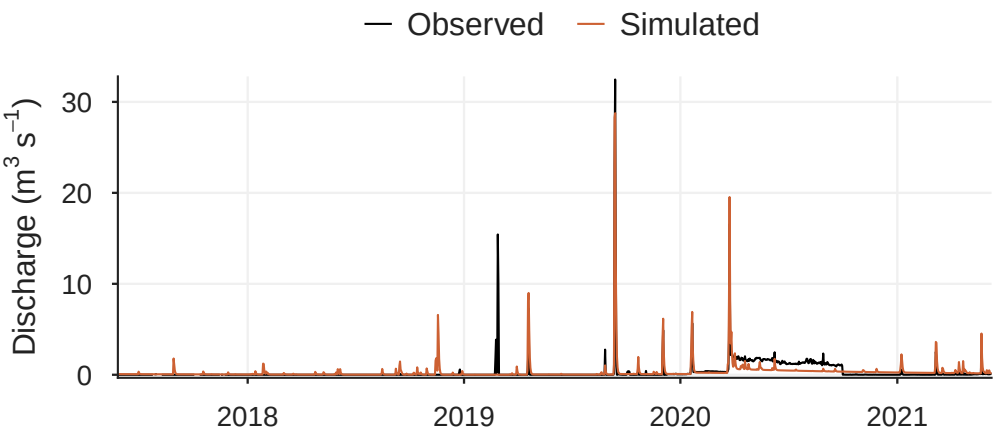

Figure S2: Discharge time series for the calibration period. The black line correspond to the observed time series and the orange line to the simulated time series.

Figures

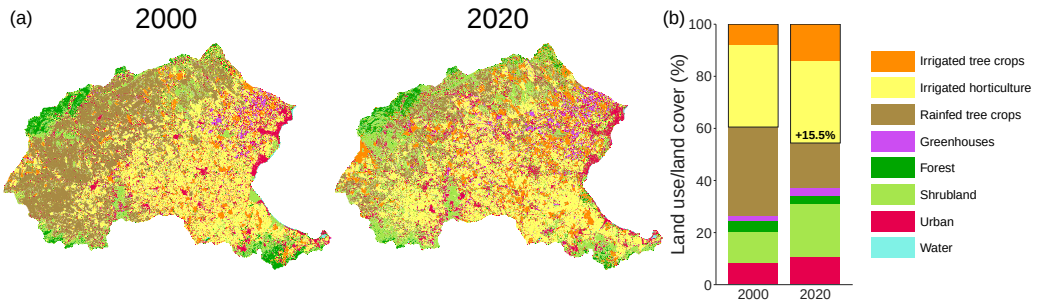

Figure S3: (a) Historical land use maps for 2000 and 2020. (b) Land use distribution (%) for the 2000 and 2020. The black boxes indicate the total irrigated area, where the percentage change indicates the change in irrigated area for 2020 with respect to 2000.

Tables

Table S4: The variables used as input for the iClue land use model.

ID	Variable	Comment/source
1	Biovar 1	Fick and Hijmans (2017)
2	Biovar 2	Fick and Hijmans (2017)
3	Biovar 3	Fick and Hijmans (2017)
4	Biovar 4	Fick and Hijmans (2017)
5	Biovar 5	Fick and Hijmans (2017)
6	Biovar 6	Fick and Hijmans (2017)
7	Biovar 7	Fick and Hijmans (2017)
8	Biovar 8	Fick and Hijmans (2017)
9	Biovar 9	Fick and Hijmans (2017)
10	Biovar 10	Fick and Hijmans (2017)
11	Biovar 11	Fick and Hijmans (2017)
12	Biovar 12	Fick and Hijmans (2017)
13	Biovar 13	Fick and Hijmans (2017)
14	Biovar 14	Fick and Hijmans (2017)
15	Biovar 15	Fick and Hijmans (2017)
16	Biovar 16	Fick and Hijmans (2017)
17	Biovar 17	Fick and Hijmans (2017)
18	Biovar 18	Fick and Hijmans (2017)
19	Biovar 19	Fick and Hijmans (2017)
20	Clay fraction	Faz Cano (2003)
21	Sand fraction	Faz Cano (2003)
22	Soil types	Faz Cano (2003)
23	DEM	Digital elevation model; Ministerio de Fomento de España (2015)
24	Slope	Ministerio de Fomento de España (2015)
25	Distance to urban	Obtained from 2020 land use map
26	Distance to water	Obtained from 2020 land use map
27	Annual precipitation	1991-2020; Peral García et al. (2017)
28	Average temperature	1991-2020; Peral García et al. (2017)
29	Irrigation districts	Confederación Hidrográfica del Segura (2015)

Table S5: Climate model characteristics of the nine GCM/RCM combinations.

GCM	CCLM[a]	HIRHAM5[b]	RACMO[c]	RCA[d]	WRF[e]
CNRM-CM5	×			×	
EC-EARTH	×	×	×	×	
IPSL-CM5A-MR					×
MPI-ESM-LR	×			×	

[a] Climate Limited-area Modelling-Community (CLMcom)

[b] Danish Meteorological Institute (DMI)

[c] Royal Netherlands Meteorological Institute (KNMI)

[d] Swedish Meteorological and Hydrological Institute (SMHI)

[e] Institut Pierre Simon Laplace (IPSL)

References

MITECO, Análisis de Soluciones Para El Vertido Cero al Mar Menor Proveniente Del Campo de Cartagena, Technical Report 07.803-0177/0411, MITECO, 2019.

Confederación Hidrográfica del Segura, Plan Hidrológico de La Cuenca Del Segura. 2022-2027, Technical Report, Confederación Hidrográfica del Segura, Murcia, Spain, 2023.

J. Jiménez-Martínez, J. García-Aróstegui, J. Hunink, S. Contreras, P. Baudron, L. Candela, The role of groundwater in highly human-modified hydrosystems: A review of impacts and mitigation options in the Campo de Cartagena-Mar Menor coastal plain (SE Spain), Environmental Reviews 24 (2016) 377–392. doi:10.1139/er-2015-0089.

Á.-F. Morote, J. Olcina, A.-M. Rico, Challenges and Proposals for Socio-Ecological Sustainability of the Tagus–Segura Aqueduct (Spain) under Climate Change, Sustainability 9 (2017) 2058. doi:10.3390/su9112058.

M. Soto-García, V. Martínez-Alvarez, P. A. García-Bastida, F. Alcon, B. Martin-Gorriz, Effect of water scarcity and modernisation on the performance of irrigation districts in south-eastern Spain, Agricultural Water Management 124 (2013) 11–19. doi:10.1016/j.agwat.2013.03.019.

J. P. C. Eekhout, J. de Vente, Assessing the effectiveness of Sustainable Land Management for large-scale climate change adaptation, Science of The Total Environment 654 (2019) 85–93. doi:10.1016/j.scitotenv.2018.10.350.

E. Aguilera, L. Lassaletta, A. Gattinger, B. S. Gimeno, Managing soil carbon for climate change mitigation and adaptation in Mediterranean cropping systems: A meta-analysis, Agriculture, Ecosystems and Environment 168 (2013) 25–36. doi:10.1016/j.agee.2013.02.003.

M. Almagro, J. de Vente, C. Boix-Fayos, N. García-Franco, J. Melgares de Aguilar, D. González, A. Solé-Benet, M. Martínez-Mena, Sustainable land management practices as providers of several ecosystem services under rainfed Mediterranean agroecosystems, Mitigation and Adaptation Strategies for Global Change 21 (2016) 1029–1043. doi:10.1007/s11027-013-9535-2.

BOE, Ley 3/2020, de 27 de julio, de recuperación y protección del Mar Menor, 2020.

K. Arora, S. K. Mickelson, M. J. Helmers, J. L. Baker, Review of Pesticide Retention Processes Occurring in Buffer Strips Receiving Agricultural Runoff, JAWRA Journal of the American Water Resources Association 46 (2010) 618–647. doi:10.1111/j.1752-1688.2010.00438.x.

R. Prosser, P. Hoekstra, S. Gene, C. Truman, M. White, M. Hanson, A review of the effectiveness of vegetated buffers to mitigate pesticide and nutrient transport into surface waters from agricultural areas, Journal of Environmental Management 261 (2020) 110210. doi:10.1016/j.jenvman.2020.110210.

W. Terink, A. F. Lutz, G. W. H. Simons, W. W. Immerzeel, P. Droogers,

SPHY v2.0: Spatial Processes in HYdrology, Geoscientific Model Development 8 (2015) 2009–2034. doi:10.5194/gmd-8-2009-2015.

J. P. C. Eekhout, W. Terink, J. de Vente, Assessing the large-scale impacts of environmental change using a coupled hydrology and soil erosion model, Earth Surface Dynamics 6 (2018) 687–703. doi:10.5194/esurf-6-687-2018.

G. H. Hargreaves, Z. A. Samani, Reference crop evapotranspiration from temperature, Applied Engineering in Agriculture 1 (1985) 96–99.

W. Heber Green, G. A. Ampt, Studies on Soil Phyics., The Journal of Agricultural Science 4 (1911) 1–24. doi:10.1017/S0021859600001441.

M. De Cáceres, N. Martin-StPaul, M. Turco, A. Cabon, V. Granda, Estimating daily meteorological data and downscaling climate models over landscapes, Environmental Modelling and Software 108 (2018) 186–196. doi:10.1016/j.envsoft.2018.08.003.

C. Romero-Trigueros, J. J. Cabañero, P. A. Tortosa, J. M. Gambín, J. F. Maestre-Valero, E. N. Nicolás, Medium-long term effects of saline reclaimed water and regulated deficit irrigation on fruit quality of citrus, Journal of the Science of Food and Agriculture 100 (2020) 1350–1357. doi:10.1002/jsfa.10091.

A. B. Mira-García, C. Romero-Trigueros, J. M. B. Gambín, M. D. P. Sánchez-Iglesias, P. A. N. Tortosa, E. N. Nicolás, Estimation of stomatal conductance by infra-red thermometry in citrus trees cultivated under regulated deficit irrigation and reclaimed water, Agricultural Water Management 276 (2023) 108057. doi:10.1016/j.agwat.2022.108057.

H. V. Gupta, H. Kling, K. K. Yilmaz, G. F. Martinez, Decomposition of the mean squared error and NSE performance criteria: Implications for improving hydrological modelling, Journal of Hydrology 377 (2009) 80–91. doi:10.1016/j.jhydrol.2009.08.003.

W. Maetens, M. Vanmaercke, J. Poesen, B. Jankauskas, G. Jankauskiene, I. Ionita, Effects of land use on annual runoff and soil loss in Europe and the Mediterranean: A meta-analysis of plot data, Progress in Physical Geography 36 (2012) 599–653. doi:10.1177/0309133312451303.

J. García-Pintado, M. Martínez-Mena, G. G. Barberá, J. Albaladejo, V. M. Castillo, Anthropogenic nutrient sources and loads from a Mediterranean catchment into a coastal lagoon: Mar Menor, Spain, Science of The Total Environment 373 (2007) 220–239. doi:10.1016/j.scitotenv.2006.10.046.

M. F. Carreño Fructuoso, Seguimiento de Los Cambios de Usos y Su Influencia En Las Comunidades y Hábitats Naturales En La Cuenca Del Mar Menor, 1988-2009, Con El Uso de SIG y Teledetección, Ph.D. thesis, Universidad de Murcia, Murcia, 2015.

S. E. Fick, R. J. Hijmans, WorldClim 2: New 1-km spatial resolution climate surfaces for global land areas, International Journal of Climatology 37 (2017) 4302–4315. doi:10.1002/joc.5086.

A. Faz Cano, El suelo de la Región de Murcia y su potencial Agrícola, in: M. Esteve Selma, M. Llorens, C. Martínez Gallur (Eds.), Los Recursos Naturales de La Región de Murcia: Un Análisis Interdisciplinar, Universidad de Murcia, Servicio de Publicaciones, Murcia, Spain, 2003, pp. 161–170.

Ministerio de Fomento de España, Plan Nacional de Ortofotografía Aérea, 2015.

C. Peral García, B. Navascués Fernández-Victorio, P. Ramos Calzado, Serie de precipitación diaria en rejilla con fines climáticos, Agencia Estatal de Meteorología, 2017. doi:10.31978/014-17-009-5.

Confederación Hidrográfica del Segura, Plan Hidrológico de La Cuenca Del Segura. 2015-2021, Technical Report, Confederación Hidrográfica del Segura, Murcia, Spain, 2015.